

The Anaphase-Promoting Complex and Separin Are Required for Embryonic Anterior-Posterior Axis Formation

Chad A. Rappleye,¹ Akiko Tagawa,¹
Rebecca Lyczak,² Bruce Bowerman,²
and Raffi V. Aroian^{1,3}

¹Section of Cell and Developmental Biology
University of California, San Diego
La Jolla, California 92093

²Institute of Molecular Biology
University of Oregon
Eugene, Oregon 97403

Summary

Polarization of the one-cell *C. elegans* embryo establishes the animal's anterior-posterior (a-p) axis. We have identified reduction-of-function anaphase-promoting complex (APC) mutations that eliminate a-p polarity. We also demonstrate that the APC activator *cdc20* is required for polarity. The APC excludes PAR-3 from the posterior cortex, allowing PAR-2 to accumulate there. The APC is also required for tight cortical association and posterior movement of the paternal pronucleus and its associated centrosome. Depletion of the protease separin, a downstream target of the APC, causes similar pronuclear and a-p polarity defects. We propose that the APC/separin pathway promotes close association of the centrosome with the cortex, which in turn excludes PAR-3 from the posterior pole early in a-p axis formation.

Introduction

Cell polarity plays a fundamental role in development. By asymmetrically localizing determinants in a cell before division, daughter cells can adopt different fates. Prominent examples include anterior-posterior (a-p) axis formation in the one-cell *Caenorhabditis elegans* embryo, *Drosophila* neuroblast determination, and animal-vegetal axis formation in *Xenopus* (Campos-Ortega, 1997; Chang et al., 1999; Kempfues et al., 1988). Polarization of these cell types, as well as the formation of tight junctions in mammalian epithelial cells, requires a group of proteins related to the *C. elegans* PAR-3, PAR-6, and atypical protein kinase C (PKC-3) proteins (Joberty et al., 2000; Nakaya et al., 2000; Wodarz et al., 1999).

In *C. elegans*, an outline of how the one-cell embryo, called P_0 , becomes polarized has emerged. Fertilization by the sperm occurs at the end opposite the oocyte pronucleus and brings in a centrosome associated with the paternal pronucleus (Albertson, 1984). The centrosome, or associated microtubules, provide a cue via interactions with the adjacent actin-rich cortex that establishes a posterior pole and defines the a-p body axis (Goldstein and Hird, 1996; Hird and White, 1993; O'Connell et al., 2000; Wallenfang and Seydoux, 2000). As a result, a PAR-3/PAR-6/PKC-3 protein complex becomes

concentrated in the anterior cortex and, reciprocally, PAR-2 becomes concentrated in the posterior cortex (Boyd et al., 1996; Etemad-Moghadam et al., 1995; Hung and Kempfues, 1999; Tabuse et al., 1998). These proteins may generate fundamental differences in the anterior and posterior of P_0 such that it divides asymmetrically into a large anterior daughter, AB, which gives rise to most of the neuroectoderm, and a smaller posterior daughter, P₁, which makes most of the mesoderm and all of the endoderm.

To better understand how factors such as PAR proteins that are strictly involved in establishing polarity interact with the basic cellular machinery, we have identified *pod*, or *polarity and osmotic defective*, genes that are required both for a-p polarity and more general cellular functions. The first gene in this new class, *pod-1*, encodes an actin binding protein asymmetrically localized at the anterior cortex of P_0 (Aroian et al., 1997; Rappleye et al., 1999). The second, *pod-2*, functions in the same pathway as *pod-1* and was identified in a screen for cold-sensitive mutants (Tagawa et al., 2001). Mutation of either *pod-1* or *pod-2* causes loss of a-p polarity in ~50% of one-cell embryos (Rappleye et al., 1999; Tagawa et al., 2001). Mutations in *pod-1* and *pod-2* also give rise to osmotically sensitive embryos, suggesting that they affect more general cell functions (e.g., membrane trafficking) required both for the production of the secreted eggshell that protects the embryo and for a-p axis formation.

Here we describe the identification and characterization of five additional *pod* loci. In these new *pod* mutants, complete disruption of a-p polarity, as judged by symmetric cleavage and mislocalization of polarized proteins, occurs in nearly all one-cell embryos. We demonstrate that these *Pod* mutant alleles represent partial loss-of-function mutations in five components of the anaphase-promoting complex (APC), and that the APC functions around the time of meiosis to establish polarity. We also show that the APC activator, *cdc20*, and the downstream protease separin are required for a-p polarity. The loss of APC and separin leads to a failure of the paternal pronucleus/centrosome to associate with the actin-rich cortex and, therefore, a failure in the transduction of the presumed polarity signal from the centrosome to the cortex. We conclude that the APC can function to regulate metazoan axis formation.

Results

Identification of New *pod* Mutants that Eliminate A-P Polarity

Pods, or *polarity and osmotic defective* mutants, are characterized by both the loss of a-p polarity in one-cell *C. elegans* embryos and the loss of osmotic protection normally conferred by an impermeable eggshell (Rappleye et al., 1999; Tagawa et al., 2001). The eggshell defect of *pod-1* and *pod-2* embryos causes them to be sensitive to the salt and pressure conditions in their environment. Due to this sensitivity, mutations in *pod* genes are likely to have been missed in previous genetic screens.

³Correspondence: raroian@ucsd.edu

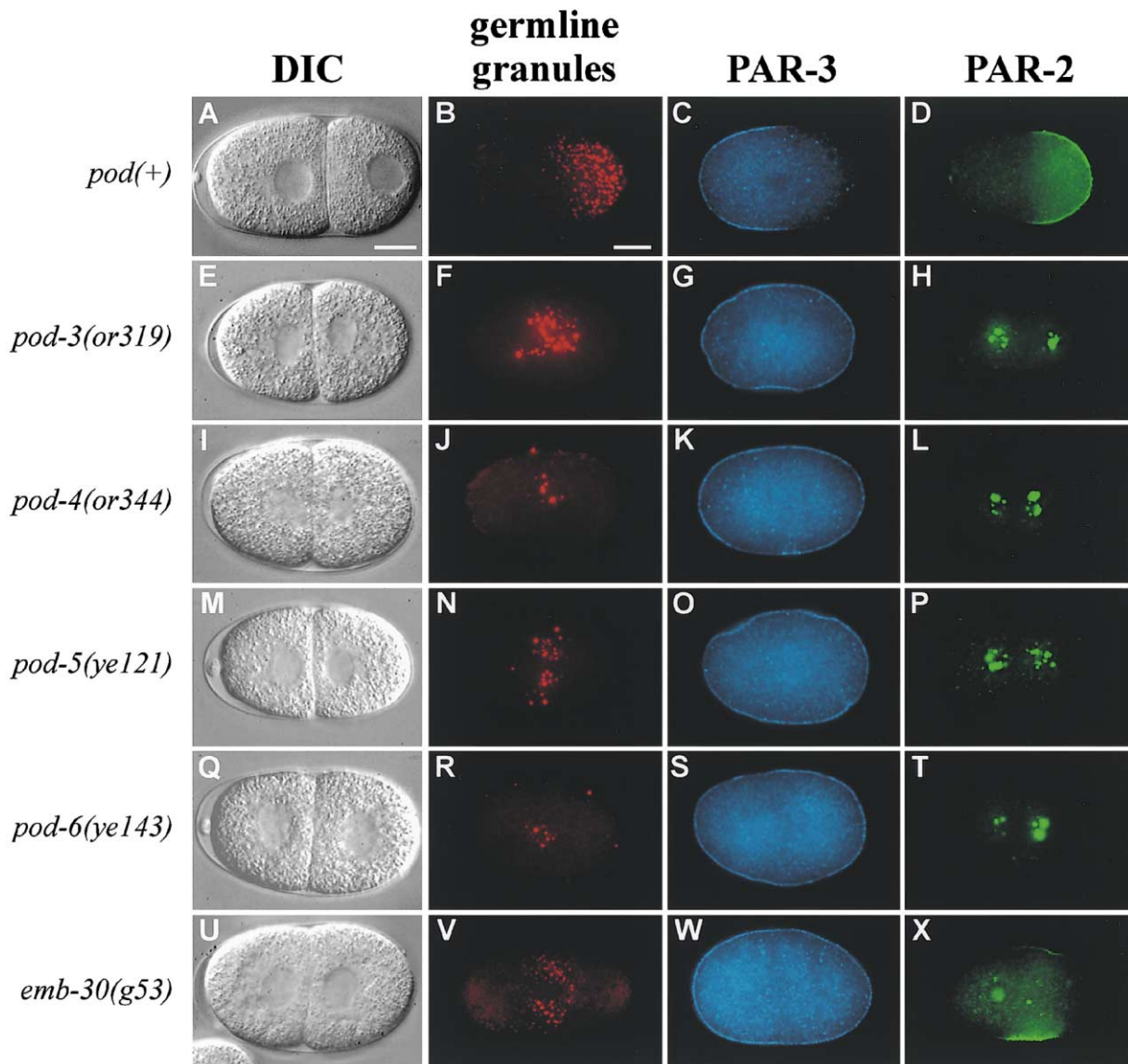


Figure 1. Loss of *pod* Gene Function Causes Loss of A-P Polarity in the One-Cell *C. elegans* Embryo P₀

Images of wild-type (A–D) and Pod mutant embryos (E–X). DIC images (A, E, I, M, Q, and U) and immunofluorescence localization of germline granules (B, F, J, N, R, and V), PAR-3 (C, G, K, O, S, and W), and PAR-2 (D, H, L, P, T, and X). All embryos are oriented with anterior to the left; all panels show a different individual embryo. Wild-type (A) divides asymmetrically, (B) segregates germline granules to the posterior, (C) restricts PAR-3 to the anterior cortex, and (D) restricts PAR-2 to the posterior cortex. *pod-3(or319)* one-cell embryos (E) divide symmetrically, (F) fail to segregate germline granules to the posterior, (G) have uniform cortical PAR-3 localization, and (H) localize PAR-2 off the cortex in cytoplasmic clusters. The same polarity defects are found in (I–L) *pod-4(or344)* mutant embryos, (M–P) *pod-5(ye121)* mutant embryos, (Q–T) *pod-6(ye143)* mutant embryos, and (U–X) *emb-30(g53)* mutant embryos. For *pod-3*, *pod-5*, and *pod-6* embryos, penetrance of phenotypes shown are $\geq 90\%$, $n = 10$ –20 embryos; for *pod-4* penetrance of phenotypes shown are $\geq 65\%$. For *emb-30* embryos, 12/19 divided symmetrically, 11/27 showed central germline granules, 4/12 showed uniform cortical PAR-3, 4/9 showed PAR-2 cytoplasmic puncta as well as lateral cortical patches. Scale bar here and elsewhere = 10 μ m.

We collected 103 osmotically sensitive embryonic mutants from existing collections and new genetic screens. Nineteen exhibited symmetric first cleavage and were found to define 10 complementation groups. Five of these loci, *pod-3*, *pod-4*, *pod-5*, *pod-6*, and *emb-30*, were selected for further study based on the high penetrance of their polarity defects (Table 1).

In a wild-type one-cell embryo, the mitotic spindle moves posteriorly during anaphase, giving rise to a larger anterior daughter cell and a smaller posterior cell (Figure

1A). In contrast, *pod-3*, *pod-4*, *pod-5*, *pod-6*, and *emb-30* mutant embryos divide symmetrically (Figures 1E, 1I, 1M, 1Q, and 1U), as do Par mutant embryos (Kemphues et al., 1988). Furthermore, both mutant daughter cells divide synchronously with transversely oriented mitotic spindles, in contrast to wild-type two-cell embryos that divide asynchronously and in orthogonal orientations (data not shown). Pseudocleavage and concurrent asymmetric cytoplasmic flows, both indicators of forming a-p polarity, are absent in Pod mutant embryos.

Table 1. Quantitation of Embryonic Defects of Pod APC Alleles

Gene	Allele	Embryo Lethality Fraction (n) ^a	Osmotic Sensitivity Fraction (n) ^a	Symmetric Two-Cell Fraction (n) ^b	Relative Area of Blastomere ^c	Fails to Complement ^d	APC Subunit ^d
<i>pod</i> (+)		0.00 (1042)	0.00 (1042)	0.00 (21)	0.57	NA	NA
<i>pod</i> -3	<i>or319</i>	1.00 (322)	1.00 (322)	1.00 (12)	0.49	<i>mat</i> -2(ax76)	APC1
	<i>or374</i>	0.93 (337)	0.57 (337)	0.40 (20)			
	<i>or385</i>	0.78 (191)	0.64 (191)	0.43 (21)			
<i>pod</i> -4	<i>or344</i>	0.96 (483)	0.91 (483)	0.82 (17)	0.50	<i>mat</i> -3(ax148)	APC8
<i>pod</i> -5	<i>ye121</i>	1.00 (591)	0.99 (478)	1.00 (11)	0.50	<i>mat</i> -1(ax227)	APC3
<i>pod</i> -6	<i>ye143</i>	0.99 (478)	0.99 (478)	1.00 (14)	0.50	<i>emb</i> -27(g48)	APC6
<i>emb</i> -30	<i>g53</i>	1.00 (150)	0.85 (150)	0.63 (19)	0.51	NA	APC4

^aHomozygous mothers were allowed to lay embryos on Nile Blue plates at nonpermissive temperature, removed, and the embryos scored 24 hr later for lack of hatching (lethality) and uptake of blue dye (osmotic sensitivity). n = number of embryos scored.

^bSingle embryos were lineaged from the one-cell to two-cell stage. The relative sizes of the blastomeres were measured just after the completion of cleavage and deemed to be symmetric if the anterior cell represented less than 53% the total area (Rappleye et al., 1999).

^cRatio of anterior blastomere surface area to total surface area in two-cell symmetric embryos. Ratio for wild-type given for comparison.

^dSee Experimental Procedures for complementation tests.

^eCorresponding APC subunit encoded by or implied to be encoded by given *pod* gene.

We next tested whether these five genes that mutate to a Pod phenotype are required for the asymmetric distribution of developmental regulatory proteins. Germline granules, a marker for germline potential, are normally segregated in a cell cycle-dependent manner to the posterior of the one-cell embryo P₀ (Figure 1B) and, thus, are inherited only by the posterior daughter, P₁ (Strome and Wood, 1983). In *pod*-3, *pod*-4, *pod*-5, *pod*-6, and *emb*-30 mutant embryos, germline granules are not segregated to the posterior and instead are clumped near the center of the embryo (Figures 1F, 1J, 1N, 1R, and 1V). These *pod* genes also are required to polarize PAR-3 and PAR-2, which establish a-p polarity and which occupy reciprocal domains at the anterior and posterior cell cortex, respectively (Figures 1C and 1D; Boyd et al., 1996; Etemad-Moghadam et al., 1995). In Pod embryos, PAR-3 is distributed uniformly throughout the cortex (Figures 1G, 1K, 1O, 1S, and 1W), whereas PAR-2 is missing from the cortex and is instead present in cytoplasmic foci clustered near microtubule organizing centers (Figures 1H, 1L, 1P, 1T, 1X, and 2G). In embryos from the less penetrant Pod mutant alleles *emb*-30(*g53*) and *pod*-4(*or344*), PAR-2 can retain reduced cortical localization that is often lateral (Figure 1X). We conclude that *pod*-3, *pod*-4, *pod*-5, *pod*-6, and *emb*-30 are required to establish the a-p body axis.

pod-3, *pod*-4, *pod*-5, *pod*-6, and *emb*-30 Encode Subunits of the APC

In the process of genetically mapping *pod*-3, -4, -5, and -6 (data not shown), we noticed the striking coincidence that each mapped to the same chromosomal interval as a *mat* gene and that the *pods* and *mat*s had the same unusual dual maternal and paternal requirements. Mutations in these *mat* genes, for metaphase-to-anaphase transition, cause one-cell embryos to arrest in metaphase of meiosis I (Golden et al., 2000). Complementation tests indeed confirmed that *pod*-3, *pod*-4, *pod*-5, and *pod*-6 are mutations in the *mat* genes *mat*-2, *mat*-3, *mat*-1, and *emb*-27, respectively (Table 1). Since this paper focuses on the polarity functions of these genes, we will retain the designation "pod" for this paper, but our alleles will be deposited using their respective *mat* and *emb* designations.

Golden et al. noted that the *mat* genes are all likely to encode components of the APC. The APC is a ubiquitin protein ligase required for the destruction of anaphase inhibitors and mitotic cyclins (Zachariae and Nasmyth, 1999). The *mat* genes *emb*-27 and *emb*-30 have been cloned and encode APC-6 and APC-4 subunits, respectively (Furuta et al., 2000; Golden et al., 2000); the remaining *mat* genes each map to a region that includes a different APC subunit (Table 1; Golden et al., 2000). To confirm that a *pod* gene encodes an APC subunit, we identified a point mutation associated with the *pod*-4(*or344*) allele in the *C. elegans* APC-8 homolog (data not shown). We also verified that partial depletion of the APC-8 homolog can reproduce the *pod*-4 mutant phenotypes (see below). Thus, *pod*-4, *pod*-6, and *emb*-30 encode APC-8, APC-6, and APC-4, respectively, and *pod*-3 and *pod*-5 are implied to encode APC-1 and APC-3, respectively.

To understand why embryos mutant for the Mat alleles of the APC arrest in meiosis I whereas embryos mutant for the Pod alleles progress through the first cell cycle with loss of polarity, we investigated the genetic relationship between the Pod and the Mat phenotypes. Our data indicates that the Pod phenotype results from a less severe reduction of function of the APC than the Mat phenotype. Reducing the copy number of a Pod APC allele by placing it in *trans* to a deficiency causes a significant increase in the number of arrested one-cell embryos (Figure 2A). Additionally, we examined the effects of a continual reduction in *pod*-4 function using RNA-mediated interference, or RNAi, mediated by feeding double-stranded RNA (dsRNA). Continual feeding of dsRNA to *C. elegans* hermaphrodites can result in the progressive depletion of a given gene's product (Kamath et al., 2000). Among one-cell embryos isolated from mothers 15–18 hr after *pod*-4 dsRNA feeding was initiated, many showed the same polarity defects as seen in *pod*-4(*or344*) mutant embryos (Figures 2B–2G). In contrast, among embryos isolated at later time points and further depleted for POD-4, a greater percentage was unable to progress through the one-cell stage (Figure 2B). Thus, the Mat phenotype is the consequence of a more severe reduction of APC function than the Pod phenotype.

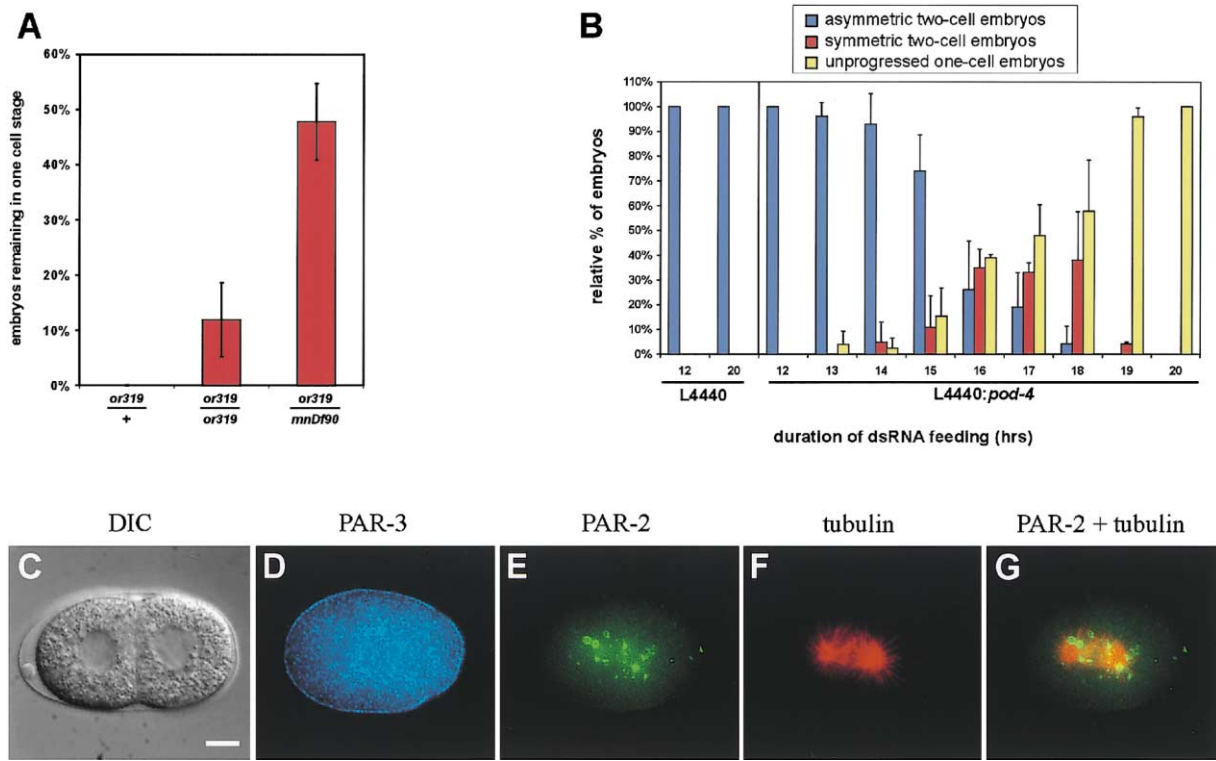


Figure 2. Loss of A-P Polarity is a Consequence of a Less Severe Reduction of Function of the APC Than of One-Cell Arrest

(A) Percentage of one-cell *pod-3(or319)* embryos remaining in the one-cell stage increases as the dose of *pod-3* is reduced. *mnDf90* is a large deficiency that spans *pod-3*.

(B) RNAi of *pod-4*. Shorter duration of dsRNA feeding results in some Pod embryos while longer duration of dsRNA feeding (more severe reduction of POD-4) results exclusively in inhibition of one-cell progression. Blue bars, asymmetric two-cell embryos; red bars, symmetric embryos; yellow bars, embryos that failed to progress past the one-cell stage. There are two to four independent experiments at each time point. L4440, empty dsRNA feeding vector; L4440: *pod-4*, feeding vector containing *pod-4* cDNA.

(C-G) Representative images of *pod-4(RNAi)* embryos showing phenocopy of the *pod-4(or344)* polarity phenotype. (C) Symmetric two-cell embryo produced after 17 hr of *pod-4(RNAi)*, (D) uniform PAR-3 around the cortex, and (E) PAR-2 mislocalized to cytoplasmic foci. (F) Tubulin staining of the same metaphase embryo in (E), and (G) merged image confirming PAR-2 foci (green) clustered around the microtubule asters (red).

Embryos Mutant for the Pod Alleles of the APC Have Slowed Mitotic and Meiotic Cell Cycles

Since the APC is required for cell cycle progression, we investigated whether Pod APC mutant embryos have altered cell-cycle timings. Pod embryos progress through mitosis in the one-cell embryo with a slight delay: wild-type embryos progress from pronuclear joining through cytokinesis in 9 ± 1 min ($n = 5$), *pod-3(or319)* embryos in 16 ± 5 min ($n = 6$), *pod-4(or344)* embryos in 13 ± 2 min ($n = 14$), *pod-5(ye121)* embryos in 14 ± 2 min ($n = 10$), and *pod-6(ye143)* embryos in 15 ± 3 min ($n = 11$).

Meiosis also takes longer in Pod mutant embryos. Mature wild-type oocytes are arrested in prophase of meiosis I (McCarter et al., 1999). Upon fertilization, the arrested maternal DNA reenters the cell cycle, completes meiosis I and initiates and completes meiosis II. The time from fertilization to the completion of meiosis II (scored as reformation of the maternal pronuclear envelope) is 29 ± 3 min ($n = 4$) in wild-type embryos versus 65 ± 7 min ($n = 7$) in *pod-3(or319)* mutant embryos. Despite delays, Pod APC mutant embryos complete both meiosis and mitosis and, apart from polarity defects, do not show other gross cellular abnormalities.

The APC Establishes Polarity during Meiosis

To determine when the APC is required for a-p polarity, we performed temperature shift studies using a temperature-sensitive allele of *pod-3*. *pod-3(or319)* mutant hermaphrodites were raised at either the permissive (15°C) or the nonpermissive (25°C) temperature, shifted to the opposite temperature for a fixed period of time, and then cut open. Two-cell embryos were scored for symmetric or asymmetric cleavage. Using this approach, the upshift and downshift curves meet just around the time of fertilization (Figure 3A), suggesting that this point is when the gene product is required. However, this approach is complicated by the fact that the cell cycle is delayed in *pod-3* embryos at 25°C , which would shift some of the downshift data points to the right and make it ambiguous as to whether the gene product is required before or after meiosis is complete.

We therefore directly tested whether *pod-3* function was required before or after meiosis by following individual embryos shifted just after meiosis had been completed. *pod-3(or319)* embryos were fertilized at the nonpermissive temperature, allowed to complete meiosis, and then immediately shifted down to the permissive temperature. These embryos all divided symmetrically

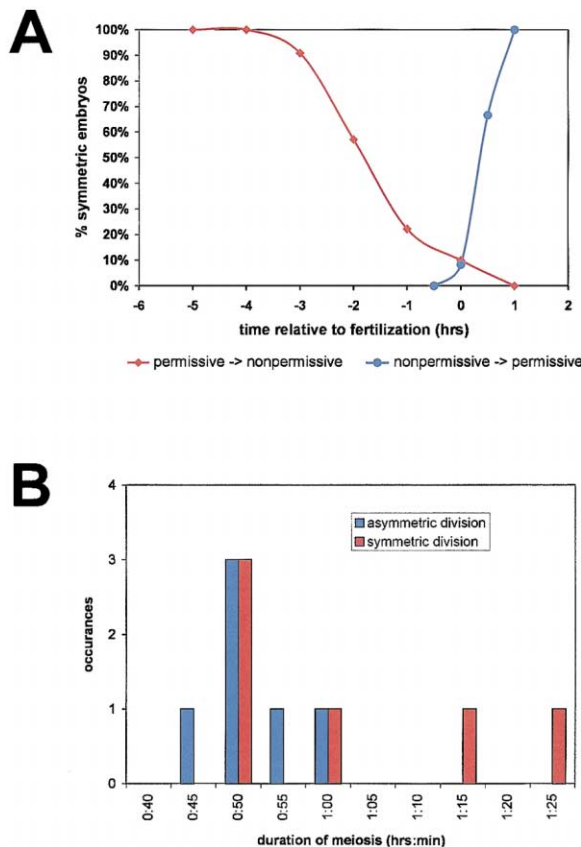


Figure 3. APC Polarity Function Is Required Around the Time of Meiosis but Is Not Linked to Meiotic Delay

(A) Results of temperature shift experiments to define the critical time period for *pod-3(or319)* for its polarity function. Times normalized to 24°C and plotted relative to fertilization ($t = 0$). Each time point represents the percentage of 9–14 two-cell embryos scored for symmetry of the first division.

(B) Meiotic delays caused by APC4 mutant are not correlated with loss of polarity. Histogram showing the number of symmetric (red) versus asymmetric (blue) two-cell embryos produced according to the duration of individual meioses (time in hr:min).

($n = 7$). Identical results were obtained for *pod-4(or344)*, *pod-5(ye121)*, and *pod-6(ye143)* ($n = 2$ for each). Conversely, *pod-3(or319)* embryos that were fertilized at the permissive temperature and shifted to the nonpermissive temperature just as meiosis completed, all divided asymmetrically ($n = 9$). Taken together, our temperature shift data are most consistent with a role for the APC after fertilization but before the completion of meiosis for establishing a-p polarity.

Since the Pod APC mutants appear to function around the time of meiosis, we tested whether or not the meiotic delay might be responsible for the polarity defects. We took advantage of the fact the Pod APC allele, *emb-30(g53)*, gives rise to ~50% symmetric cleavage. We followed 12 *emb-30(g53)* embryos from the moment of fertilization to the completion of the first cleavage to see if there was a correlation between loss of polarity and meiotic delay. Although on average meiosis took longer to complete in symmetrically dividing as compared to asymmetrically dividing embryos (58 ± 14 min

versus 48 ± 5 min, $n = 6$ for each), there was poor correlation between individual meiosis times and polarity defects (Figure 3B)—four of the six embryos that divided symmetrically (red bars) showed similar meiotic delays as the embryos that divided asymmetrically (blue bars). Other aspects of meiosis appeared relatively normal—polar bodies are readily evident in many *pod* mutant embryos, and the nuclear envelope reforms properly following meiosis. These data suggest that the meiotic delay itself does not cause polarity defects. Indeed, we have been able to more fully separate polarity defects from meiotic cell cycle defects (see below).

Ubiquitin and the APC Activator *cdc20* Are Required for Polarity

Since the APC had not been previously implicated in the generation of polarity, we tested whether this role involved known APC functions. The APC functions as part of a large E3 ligase to add ubiquitin onto inhibitors of cell cycle progression, targeting them for degradation and allowing the cell cycle to progress (Zachariae and Nasmyth, 1999). To determine whether ubiquitination by APC might be involved in polarity, we performed RNAi of ubiquitin. *C. elegans* possesses one polyubiquitin gene and one monoubiquitin gene (*ubq-2*), which has ~85% nucleotide identity to each of the polyubiquitin units. Depletion of *ubq-2* by dsRNA feeding caused pleiotropic defects during the first cell cycle, making live analysis difficult. We therefore examined *ubq-2*-depleted embryos (10–13 hr post feeding) by fixation and staining with PAR-2, PAR-3, and tubulin antibodies and with DAPI (DNA). Of 34 embryos ascertained to be between the stages of pronuclear meeting and anaphase, 10 showed polarity defects. Many of these were reminiscent of Pod APC mutant embryos, namely failure to properly restrict PAR-3 from the posterior and collapse of PAR-2 around the centrosomes (Figures 4A–4C), consistent with APC polarizing the one-cell embryo P_0 via its role as a ubiquitin ligase.

The function of APC in controlling the cell cycle requires activation by binding to either the *Cdc20* or *Cdh1* activators that appear to act by physically linking the APC to substrates targeted for degradation (Pfleger et al., 2001). To test if *cdc20* is involved in the polarity role of APC, we used dsRNA feeding to progressively deplete the *C. elegans* *cdc20* homolog. As with *pod-4* dsRNA feeding experiments, we found that the mutant phenotypes became more severe over time (Figure 4D). Many embryos isolated 18–21 hr after feeding was initiated were osmotically sensitive and showed symmetric cleavage and PAR-2 mislocalization similar to that found in APC mutants (Figures 4E and 4F). As *cdc20* was further depleted (embryos isolated >22 hr after feeding was initiated), the majority of embryos failed to progress through the one-cell stage. RNAi feeding experiments with *cdh1* failed to produce any embryonic lethality. Thus, the *cdc20* activator of the APC is also required to establish a-p polarity.

PAR-3 Prevents Cortical Association of PAR-2 in an APC Mutant

As noted above, in embryos mutant for the Pod alleles of the APC, PAR-3 is uniformly distributed around the

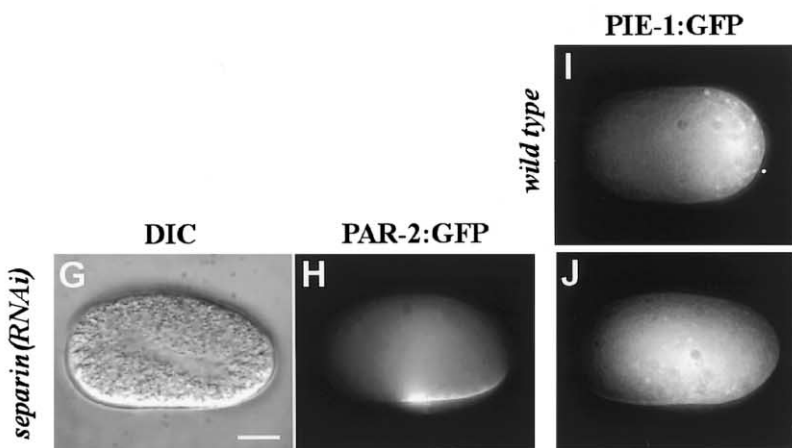
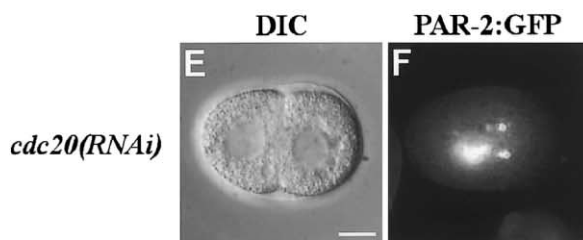
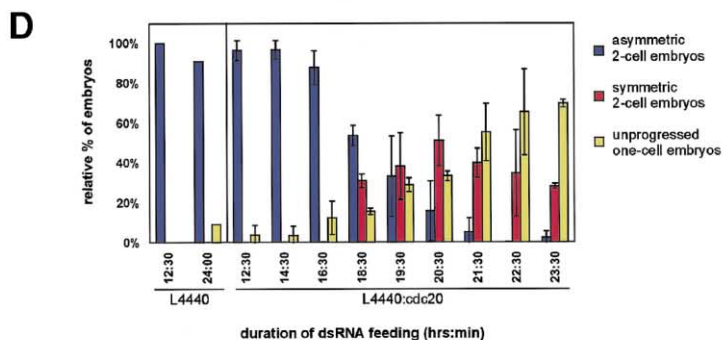
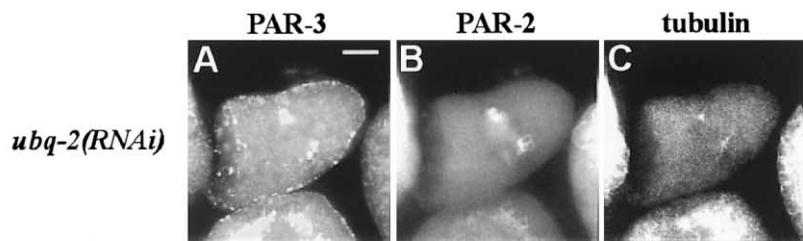


Figure 4. A-P Polarity Requires Other Components of the APC Pathway, i.e., Ubiquitin (A-C), the APC Activator *cdc20* (D-F), and Separin (G-J)

(A-C) Triple staining of a one-cell embryo in prometaphase depleted of ubiquitin by RNAi showing (A) PAR-3 uniformly localized around the cell cortex, (B) PAR-2 mislocalized to cytoplasmic foci, and (C) microtubule staining.

(D-F) RNAi of the *C. elegans* *cdc20* homolog phenocopies polarity defects of APC mutants.

(D) Graph showing the time course of production of symmetric embryos (as Figure 2B).

(E) A symmetric two-cell embryo from a hermaphrodite fed *cdc20* dsRNA for 20 hr.

(F) Same embryo as in (E) at an earlier time (metaphase, one-cell) showing mislocalization of PAR-2:GFP to cytoplasmic foci.

(G) DIC image showing an embryo depleted of separin with the anaphase spindle positioned centrally relative to the a-p axis.

(H) Same embryo as in (G) showing PAR-2 mislocalized to a small patch on the lateral cortex.

(I) PIE-1:GFP in a wild-type one-cell anaphase embryo properly segregated to the posterior.

(J) PIE-1:GFP in a separin RNAi one-cell anaphase embryo showing lack of polarization to the posterior.

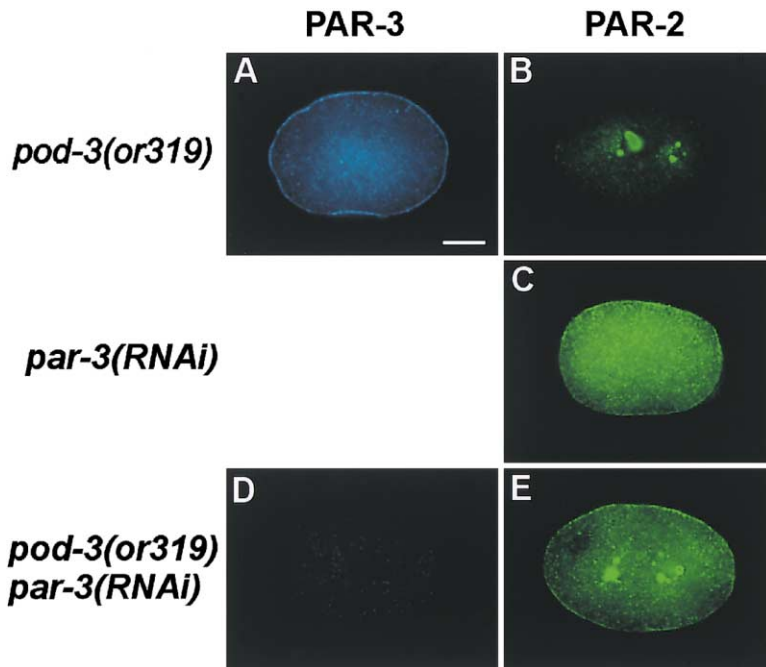


Figure 5. PAR-3 Prevents Association of PAR-2 with the Cortex in APC Mutant Embryos

(A and D) PAR-3 localization in one-cell mutant embryos.

(B, C, and E) PAR-2 localization in one-cell mutant embryos.

In a *pod-3* mutant embryo, (A) PAR-3 is uniform around the cortex whereas (B) PAR-2 is absent from the cortex and present only as cytoplasmic foci. (C) When PAR-3 is depleted by RNAi, PAR-2 is uniform at the cortex. Removal of PAR-3 (D) from *pod-3* mutant embryos allows PAR-2 (E) to associate with the cortex.

cortex and PAR-2 is present only as cytoplasmic foci (Figures 5A and 5B). In contrast, in embryos mutant for *par-3* alone, PAR-2 is still found at the cortex, albeit uniformly (Figure 5C; Etemad-Moghadam et al., 1995). Given that *par-2* and *par-3* are thought to act antagonistically to each other (Guo and Kemphues, 1996), we tested whether cortical PAR-3 was excluding PAR-2 from the cortex in Pod/APC mutant embryos. After depleting PAR-3 in Pod/APC mutant embryos, PAR-2 returns to the cortex in a uniform, nonpolarized distribution (Figures 5D and 5E). Thus, in an APC mutant embryo, uniform PAR-3 excludes PAR-2 from the cortex. Since in wild-type PAR-3 is initially symmetric around the cortex but becomes asymmetric by meiosis II (Etemad-Moghadam et al., 1995), we conclude that the APC normally functions to restrict PAR-3 to the anterior, allowing cortical association of PAR-2 at the posterior.

The Paternal Pronucleus that Brings in the Polarity Cue Behaves Abnormally in APC, but Not *par-3*, Mutant Embryos

How might the APC limit PAR-3 to the anterior? Microtubule interactions with the cortex and a functional centrosome appear to play important roles in dictating the localization of PAR-2 at the cortex (O'Connell et al., 2000; Wallenfang and Seydoux, 2000). The centrosome is donated by the sperm and is attached to the paternal pronucleus during pronuclear stage one-cell embryos. We have characterized the behavior of the paternal pronucleus/centrosome complex (Figure 6A). It becomes discernible toward the completion of meiosis II, sometimes in the very posterior or sometimes along a lateral edge near the posterior (Figure 6A1). Before the end of meiosis (50 ± 20 s [$n = 8$]), the paternal pronucleus/centrosome becomes tightly associated with the cortex such that no cytoplasmic granules are seen between it and the embryonic cortex (Figure 6A2). Regardless of

its initial position, the paternal pronucleus and its centrosome move to the very posterior cortex just before (5/8 embryos; Figure 6A3) or within 21 s after (3/8 embryos) the end of meiosis. The pronucleus remains attached at the cortex for $4 \text{ min } 23 \pm 52$ s (relative to meiosis completion), after which it dissociates (Figure 6A4) and meets the maternal pronucleus in the posterior cytoplasm (Figure 6A5). Subsequently, the mitotic spindle forms and becomes posteriorly displaced (Figure 6A6), leading to asymmetric cleavage (Figure 6A7).

The behavior of the paternal pronucleus/centrosome complex is markedly altered in *pod-3(or319)* mutant embryos ($n = 4$; Figure 6B). After appearing, the paternal pronucleus neither tightly associates with the cortex (Figures 6B1 and 6B2) nor moves to the very posterior (Figure 6B3). Following pronuclear migration (Figure 6B4), it meets the maternal pronucleus in the center of the embryo (Figure 6B5), after which the embryo divides symmetrically (Figures 6B6 and 6B7). Thus, in embryos reduced for APC function, the characteristic close contact between the paternal pronucleus/centrosome and the embryonic cortex is absent during the early stages of polarity establishment.

We speculate that a close association of the sperm pronucleus and its centrosome with the cortex is required for specifying a posterior pole and thus required for excluding PAR-3. This model predicts that PAR-3, though affected by the centrosome-cortical interaction, should not be required for it. Indeed, in *par-3* mutant embryos the paternal pronucleus behaved as in wild-type ($n = 5$; Figure 6C). It was tightly associated with the cortex on average 60 ± 48 s before the maternal pronucleus reformed (Figure 6C2), and full posteriorization occurred before or within 35 s of the completion of meiosis II (Figure 6C3). The paternal pronucleus remained there on average $4 \text{ min } 21 \pm 28$ s prior to dissociating (Figure 6C4) and meeting the maternal pronucleus

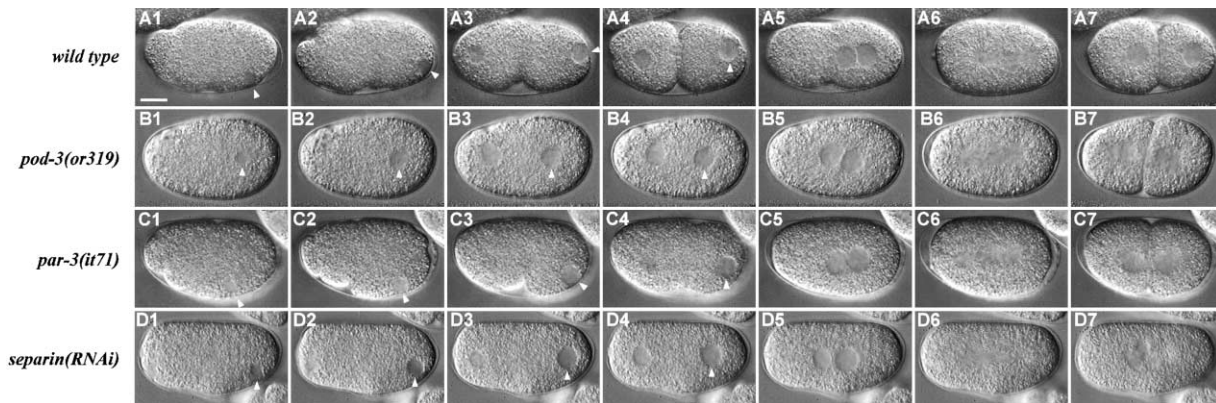


Figure 6. Cortical Association and Posterior Positioning of the Paternal Pronucleus Is Prevented by Reducing APC and Separin Function

White arrowheads indicate the paternal pronucleus.

(A) In wild-type, the paternal pronucleus (A1 and A2) tightly associates with the cortex around the time meiosis completes, (A3) moves to the very posterior cortex, and remains there for a few minutes before (A4) dissociating from the cortex (pseudocleavage is evident at this time) and (A5) meeting the maternal pronucleus in the posterior cytoplasm. (A6 and A7) Subsequent division is asymmetric.

(B1–B7) In *pod-3(or319)*, the paternal pronucleus fails to tightly associate with the cortex or to move posteriorly and meets the maternal pronucleus in the center. Subsequent division is symmetric. Tubulin staining indicates that the centrosome in *pod-3* mutant embryos is attached normally to the paternal pronucleus during pronuclear migration (not shown), implying that it is also attached to the pronucleus during earlier stages when it is more difficult to visualize.

(C1–C7) In *par-3(it71)*, the paternal pronucleus associates with the cortex, moves to the posterior, and remains there for a few minutes, like in wild-type. Subsequent division is symmetric.

(D1–D7) The paternal pronucleus in separin RNAi embryos, like in *pod-3(or319)* embryos, does not tightly associate with the cortex and does not move to the posterior, instead remaining in the posterior cytoplasm. The two pronuclei meet near the center of the embryo. The anaphase spindle elongates but does not become posteriorly displaced, setting up a symmetric division. However, cytokinesis does not occur and multiple micronuclei reform.

(Figure 6C5). These *par-3* mutant embryos subsequently divided symmetrically (Figures 6C6 and 6C7).

The Protease Separin Is Also Involved in Establishing A-P Polarity

APC^{ccdc20} targets several substrates for destruction, one of which is Pds1/securin. Removal of securin leads to activation of the protease Esp1/separin, which in turn is required in yeast for chromosome separation, stabilization and integrity of the mitotic spindle microtubules, and proper localization of the spindle pole body (Nasmyth et al., 2000; Pellman and Christman, 2001; Sullivan et al., 2001). We hypothesized that the APC might be influencing association of the paternal pronucleus/centrosome complex with the cortex through activation of separin. We therefore depleted a *C. elegans* separin homolog by feeding dsRNA and followed the behavior of the paternal pronucleus/centrosome complex in embryos isolated 14–16 hr after feeding was initiated. In these embryos, the behavior of the paternal pronucleus resembled that of the *pod-3* mutant (Figure 6D). In 17/18 embryos, the paternal pronucleus failed to move to the posterior-most cortex from an initial lateral position (Figures 6D1 and 6D2). Furthermore, in nine embryos the paternal pronucleus did not tightly associate with the cortex; cytoplasmic granules were evident juxtaposed between it and the embryonic cortex (Figures 6D3 and 6D4). In other embryos where the paternal pronucleus did become tightly associated with the cortex (either in the very posterior or laterally), it prematurely dissociated in less than 2 min following completion of meiosis. The paternal and maternal pronuclei often meet in the center

of separin RNAi embryos (Figure 6D5). The mitotic spindle sometimes remains symmetric (Figure 6D6). Cytokinesis usually fails at the end of the first cell cycle (Figure 6D7) but occurs in subsequent attempts (see Experimental Procedures). Thus, separin is required for proper association of the paternal pronucleus with, and movement along, the embryonic cortex.

Our model also predicts that separin RNAi embryos should display polarity defects. Indeed, embryos depleted of separin showed defects consistent with loss of a-p polarity. Although not all embryos were simultaneously scored for all defects, out of 67 separin RNAi embryos, we found 37 that lacked pseudocleavage and 14 that lacked cytoplasmic flows, two processes characteristic of a-p polarity. Furthermore, in six embryos, the spindle set up and remained symmetrically positioned around the middle of the embryo, sometimes aligned along the a-p axis (Figure 6D6), sometimes skewed laterally (Figure 4G). In all these cases, the posterior movement of the posterior aster during anaphase was missing. In two cases where cytokinesis completed during the first cell cycle, the daughter blastomeres divided synchronously and transversely.

To further analyze the role of separin in a-p polarity, we analyzed PAR-2:GFP and PIE-1:GFP distribution during anaphase in separin-depleted live one-cell embryos (PIE-1 is required for germline fate, and PIE-1:GFP, like germline granules, localizes to the posterior of the one-cell embryo; Figure 4I; Reese et al., 2000). Eleven of 26 embryos analyzed for PAR-2:GFP showed lateral and cortical PAR-2 localization similar to that observed in some *emb-30* and *pod-4* mutant embryos (Figure 4H; compare to Figure 1X). In five of these, PAR-2:GFP also

was found in cytoplasmic puncta, similar to that of Pod APC mutant embryos. PIE-1:GFP was also missegregated. Only five of 23 separin-depleted embryos showed wild-type segregation of PIE-1:GFP. In 11 embryos, PIE-1 failed to localize to the very posterior but instead was found near the center of the a-p axis (Figure 4J); in the remaining seven, PIE-1:GFP was largely dispersed, sometimes with a posterior bias. These data demonstrate that depletion of separin leads to a-p polarity defects, analogous to depletion of APC^{cdc20}. Since the polarity defects are not as penetrant as those associated with Pod alleles of the APC, it is possible that depletion by RNAi is less efficient at generating loss of polarity than our Pod alleles and/or that the APC has some polarity functions independent of separin.

Although polarity was affected in separin RNAi embryos, there was no change in the timing of meiosis, consistent with the fact mutation of separin in *S. pombe* does not affect cell cycle timing (Hirano et al., 1986). For separin RNAi embryos with symmetric spindles, the time from fertilization to appearance of the maternal pronucleus was 30 min 6 s \pm 1 min 40 s ($n = 5$); for other separin RNAi embryos, meiosis took 31 min 20 s \pm 2 min 32 s. Both are statistically the same as wild-type. Thus, disruption of a-p polarity caused by loss of separin cannot be a consequence of meiotic delay.

Discussion

The anterior-posterior (a-p) axis in *C. elegans* is defined by asymmetries that occur in the one-cell embryo. Although there has been significant study of proteins specifically involved in generating this polarity, there has been a relative lack of information as to how these proteins are coupled to the general cell machinery and as to the role the cell machinery plays in generating asymmetry.

Here we show that the multisubunit anaphase-promoting complex (APC) and its activator *cdc20* are required for establishing the *C. elegans* anterior-posterior axis. This finding represents a novel example of a role for the APC outside of cell cycle control. This role was first suggested by our identification of mutations in four individual APC subunits that cause loss of a-p polarity in nearly all embryos but do not cause cell cycle arrest. Our data indicate that the APC restricts PAR-3 to the anterior, subsequently allowing PAR-2 to associate with the posterior cortex. We have also been able to reproduce the polarity defects seen in APC mutants by depleting *cdc20*, and to some extent ubiquitin and the downstream component separin, indicating that a known APC pathway establishes a-p polarity. We have also demonstrated the APC and separin are required to promote a tight association between the paternal pronucleus/centrosome complex and the actin-rich cortex, and we suggest that loss of this close association accounts for the loss of polarity.

Although our results clearly indicate that APC function is required for establishing a-p polarity, it is important to consider whether the APC is playing a direct role in this process or whether the polarity defects seen in Pod mutant embryos are an indirect consequence of the osmotic sensitivity or prolonged meiosis of these mutants. Osmotic sensitivity, a consequence of defects in

the extracellular eggshell, is unlikely to cause the loss of polarity in our APC mutants. We note that only a small portion (19/103) of all osmotically sensitive mutants found in our screens have polarity defects, and we have previously reported on two other osmotic embryonic mutants, *emb-14* and *emb-20*, that do not show loss of a-p polarity (Rappleye et al., 1999; Tagawa et al., 2001). Thus, osmotic sensitivity does not lead to nonspecific loss of a-p polarity. In addition, all experiments were carried out in isotonic buffers that are sufficient to support the development of blastomeres free of the eggshell and that do not perturb the polarity of non-Pod osmotic mutants (Rappleye et al., 1999; Shelton and Bowerman, 1996). Indeed, wild-type embryos are naturally osmotically sensitive up to \sim 4–5 min before the completion of meiosis, and newly fertilized wild-type embryos put into our isotonic buffer proceed through meiosis and mitosis with the same timings, cellular events, and polarity as wild-type embryos in utero (C.A.R. and R.V.A., unpublished data). These data clearly demonstrate that neither a permeable eggshell nor the buffer used in our experiments causes defects in polarity. Along these lines, permeabilization of the eggshell (independent of an osmotically sensitive mutant) by abrasion or by strafing with a laser is also not sufficient to alter asymmetry in a one-cell embryo placed in isotonic buffers (Hill and Strome, 1988; Junkersdorf and Schierenberg, 1992).

Abnormalities in the completion of maternal meiosis, the time during which the APC appears to be acting, are also unlikely to nonspecifically cause polarity defects. In *emb-30/APC-4* mutant embryos, the length of meiotic delay does not correlate with loss of polarity. Reduction of separin by RNAi results in loss of polarity but not a meiotic delay, thereby separating loss of polarity from meiotic delay. Perturbing meiosis itself is not sufficient to perturb polarity as *mei-1* mutant embryos display severe problems in the segregation of meiotic chromosomes but retain normal polarity (Mains et al., 1990). Nor does elimination of other cell cycle proteins involved in meiosis lead to polarity defects. RNAi of a *C. elegans* cyclin-dependent kinase regulator, *cks-1*, results in a meiotic spindle that persists throughout the cell cycle, a failure to reform the maternal pronucleus, and chromosomal morphology defects (Polinko and Strome, 2000); RNAi of *cdc-25* results in delays in meiotic streaming and meiotic spindle defects, extra oocyte pronuclei, and abnormal chromatin content (Ashcroft et al., 1999). In neither case was a-p polarity significantly perturbed (occasional symmetric cleavage associated with *cdc25* RNAi was attributed to an abnormally large polar body). The high penetrance and complete loss of polarity seen in Pod APC mutant alleles, together with our finding that five APC subunits and *cdc20* mutate to the same phenotype, indicate that APC^{cdc20} functions directly in establishing a-p polarity.

A Model for the APC^{cdc20} in Generating A-P Polarity

How does APC^{cdc20} function in the generation of polarity? We suggest the following model. During meiosis II, perhaps at the metaphase to anaphase transition when the APC is known to act, APC^{cdc20} activates separin in the one-cell embryo. Separin in turn promotes tight association between the paternal pronucleus/centrosome with

the embryonic actin-rich cortex and also directs pronuclear/centrosome movement to the very posterior of the embryo. The closely positioned centrosome is able to interact with the posterior cortex and displace the PAR-3/PAR-6/PKC-3 complex, enabling PAR-2 to bind there and establishing anterior versus posterior cortical domains. Indeed, PAR-3 and PAR-6 become restricted anteriorly at roughly the same time as we observe tight association between the paternal pronucleus and the cortex (Etemad-Moghadam et al., 1995; Hung and Kemphues, 1999). Such a requirement for a tightly positioned interaction potentially explains why drugs that inhibit microtubules fail to cause polarity defects in *C. elegans* (Strome and Wood, 1983)—short-range interactions might not be affected by these drugs. Interestingly, the separin pathway in yeast is similarly required to maintain spindle pole bodies close the cortex (Sullivan et al., 2001).

How does this model account for recent observations of polarity and microtubule defects in the stronger Mat APC mutant alleles or in *spd-2* mutants (O'Connell et al., 2000; Wallenfang and Seydoux, 2000)? Mat APC mutant embryos display a small anterior patch of cortical PAR-2 and anteriorly localize the germline component PIE-1. This reversal in polarity is thought to be the result of the arrested and frayed meiotic spindle. Microtubules from this spindle abnormally and persistently contact the cortex, thereby providing a surrogate signal that repels PAR-3 and establishes PAR-2 at the anterior. Conversely, in a Pod APC mutant embryo, the meiotic spindle does not arrest, and such abnormal anterior microtubule-cortex interactions are presumably missing. Thus, the polarity reversal in Mat alleles of the APC can be attributed to an ectopic microtubule-cortex interaction at the anterior, whereas polarity loss in Pod alleles of the APC can be attributed to a lack of centrosome/microtubule-cortex interactions at either end. In *spd-2* mutant embryos, a maternal component is missing that compromises centrosome function, resulting in a delay of its ability to nucleate microtubules. As a result, polarity is perturbed, e.g., PAR-2 is often found at both poles or at the anterior end. We propose that the reduced functionality of the centrosome in the *spd-2* mutant allows enhancement of the meiotic spindle or other anterior microtubules that direct anterior localization of PAR-2. In some embryos, the reduced centrosome function might still be sufficient to promote some posterior association of PAR-2, accounting for those embryos in which dual localizations are observed. In Pod APC mutant embryos, microtubule enhancements at the anterior would be missing because the centrosome is still functional, just not at the cortex.

Given the conserved function of the APC in eukaryotes and known conservation between polarization of the *C. elegans* embryo and other cells (i.e., the PAR-3/PAR-6/PKC-3 complex), it seems likely that this system will be used in other polarization contexts. That the APC plays an important cellular function outside of the cell cycle perhaps is not unexpected given the complexity of its composition. Continued study of the APC in genetically tractable systems should help elucidate its multi-functional roles.

Experimental Procedures

Culture of *C. elegans* strains, mutagenesis, and complementation tests were performed using standard techniques (Brenner, 1974). All Pod mutant alleles are temperature-sensitive mutants. They were maintained at permissive temperature (15°C) and moved to nonpermissive conditions (24°C–25°C) as L4-staged hermaphrodites overnight to produce mutant phenotypes in the embryos. Maternal requirements were determined by mating *plg-1(e2001)*; *him-5(e1490)* males into *pod/pod* hermaphrodites at permissive and nonpermissive temperatures: at 15°C, 163/179, 111/120, 296/344, and 157/160 embryos hatched for *pod-3(or319)*, *pod-4(or344)*, *pod-5(ye121)*, and *pod-6(ye143)* mothers, respectively; at 25°C, 0/142, 14/294, 0/176, and 0/191 embryos hatched, respectively. For the paternal requirement, *pod/pod*; *him-5(e1490)/+* males were mated to *unc-4(e120)* hermaphrodites at the nonpermissive temperature, and embryo viability was scored. The number of embryos that hatched was 497/502, 49/519, 62/608, 99/380, 342/753, and 35/184 for *pod(+)*, *pod-3(or319)*, *pod-4(or344)*, *pod-5(ye121)*, and *pod-6(ye143)* males, respectively.

Identification of Pod Mutants

Osmotically sensitive (osmosensitive) embryonic lethals were collected from the *Caenorhabditis* Genetics Center (CGC) stock of published mutants (Riddle et al., 1997), from published mutants identified on chromosome III (Gönczy et al., 1999), and from a large-scale screen for temperature-sensitive embryonic lethal mutants (Encalada et al., 2000). Osmosensitive phenotypes were verified by swelling of blastomeres when embryos were placed in hypotonic media and/or uptake of Nile Blue A dye. We also devised and executed a directed genetic screen for osmosensitive lethals. *unc-52(e669)* animals were mutagenized with EMS and grown at 15°C for two generations. Synchronized F2 L1-staged hermaphrodites were plated onto plates containing 33 ng/ml Nile Blue A and shifted to 25°C at the L4 stage. Potential osmosensitive mutants were identified as those with blue-staining embryos piled next to the paralyzed *unc-52* hermaphrodite, picked individually to new plates, and recovered at 15°C. Mutants were outcrossed to N2 Bristol at least four times.

To identify osmosensitive embryos with polarity defects, mutant embryos were dissected out into isotonic embryonic blastomere growth medium (EBGM) (Shelton and Bowerman, 1996) and scored. Those alleles producing at least 2 out of 12 symmetric two-cell embryos (confirmed by measuring the cross-sectional areas at the two-cell stage) were kept as Pods.

mat complementation testing was performed by mating *mat/+* males into marked (Dpy or Unc) *pod* hermaphrodites at 25°C and looking for osmosensitive embryos from 50% of the cross progeny. *pod-3/Df* data were collected by mating *unc-4(e120)* *pod-3(or319)*; *pod-3(or319)* males into *mnDf69 unc-4(e120)/mnC1* hermaphrodites and examining the embryos produced by Unc cross progeny.

Microscopy and Immunofluorescence of *pod* Mutants

For all live observations, embryos were released and mounted in EBGM; they were maintained pressure-free by placing petroleum jelly around the edges of the coverslip. Embryos were observed with 100× DIC optics. First cell cycle times were calculated from the point of pronuclear convergence to the completion of the first cytokinesis. Meiotic timings were obtained by following embryos from the point of entry of an oocyte in the spermatheca to the reformation of the maternal pronuclear envelope. To observe fertilization, gravid hermaphrodites were emptied of previously fertilized embryos by serotonin, anesthetized in 0.1% tricaine/0.01% tetramisole, and mounted for microscopy. Fertilization was scored as passage of the proximal oocyte through the spermatheca. Newly fertilized embryos were then dissected from the hermaphrodite and mounted as above.

Immunolocalization of germline granules (O1C1D4), PAR-3, and PAR-2 were performed as described (Boyd et al., 1996; Etemad-Moghadam et al., 1995), except that embryos were dissected from gravid hermaphrodites in EBGM. All embryos were costained for microtubules using tubulin antibody DM1a to ensure they were in the first cell cycle. PAR-3 and PAR-2 costainings of *pod-4(RNAi)*

and *ubq-2(RNAi)* and PAR-2 stainings of *cdc-20(RNAi)* fixed embryos were done, for PAR-3, using an affinity-purified antibody generated against a C-terminal PAR-3 peptide and, for PAR-2, using fluorescence of PAR-2:GFP (Wallenfang and Seydoux, 2000), which is preserved during the 5 min MeOH fixation. Immunofluorescent images of embryos were collected in 0.8 μ m stacks and deconvolved using a DeltaVision system (Applied Precision) on an Olympus IX-70 microscope (60 \times , 1.40 NA objective).

RNA Interference (RNAi)

RNAi was performed by plating L4 hermaphrodites onto NG plates containing 1 mM IPTG seeded with *E. coli* (HT115/DE3) transformed with the dsRNA expressing plasmid (L4440) containing the appropriate *C. elegans* sequences (Kamath et al., 2000; Timmons and Fire, 1998). Open reading frames are as follows: *pod-4* = F10C5.1, *cdc20* = ZK177.6, *cdh1* = ZK1307.6, *ubq-2* = ZK1010.1, *separin* = Y47G6A.12. Primer sequences are available upon request. Three to four hermaphrodites were dissected in embryonic blastomere media and all one-cell embryos were monitored by DIC microscopy for the production of symmetric two-cell embryos over the course of 60 min. In separin RNAi embryos, cytokinesis often fails in the first cell cycle but completes in the second next cell cycle, a defect not seen in our other mutants. To ensure our analysis included only one-cell separin RNAi phenotypes, all separin DIC and GFP data were collected from live one-cell embryos starting from meiotic or pronuclear migration stages.

Acknowledgments

We thank Dr. Ken Kemphues for PAR antibodies, Dr. Heinke Schnabel for osmotic mutant strains, and Dr. Geraldine Seydoux for mat alleles. We thank Dr. Jim Posakony, Dr. Steve Reed, Dr. Tim Schedl, and Dr. Susan Strome for helpful discussions and Dr. Craig Hunter for pointing out that GFP fluorescence survives methanol fixation. Some *C. elegans* strains were supplied by the Caenorhabditis elegans Genetics Center, which is supported by the NIH. This work was supported by grants to R.V.A. from the National Science Foundation (IBN, 9808911) and the March of Dimes, and to B.B. from the NIH (GM49869). C.A.R. is a Howard Hughes predoctoral fellow; R.L. is an American Cancer Society Fellow.

Received November 6, 2001; revised December 31, 2001.

References

Albertson, D.G. (1984). Formation of the first cleavage spindle in nematode embryos. *Dev. Biol.* 101, 61–72.

Aroian, R.V., Field, C., Pruliere, G., Kenyon, C., and Alberts, B.M. (1997). Isolation of actin-associated proteins from *Caenorhabditis elegans* oocytes and their localization in the early embryo. *EMBO J.* 16, 1541–1549.

Ashcroft, N.R., Srayko, M., Kosinski, M.E., Mains, P.E., and Golden, A. (1999). RNA-Mediated interference of a *cdc25* homolog in *Caenorhabditis elegans* results in defects in the embryonic cortical membrane, meiosis, and mitosis. *Dev. Biol.* 206, 15–32.

Boyd, L., Guo, S., Levitan, D., Stinchcomb, D.T., and Kemphues, K.J. (1996). PAR-2 is asymmetrically distributed and promotes association of P granules and PAR-1 with the cortex in *C. elegans* embryos. *Development* 122, 3075–3084.

Brenner, S. (1974). The genetics of *Caenorhabditis elegans*. *Genetics* 77, 71–94.

Campos-Ortega, J.A. (1997). Asymmetric division: dynastic intricacies of neuroblast division. *Curr. Biol.* 7, 726–728.

Chang, P., Perez-Mongiovi, D., and Houlston, E. (1999). Organisation of *Xenopus* oocyte and egg cortices. *Microsc. Res. Tech.* 44, 415–429.

Encalada, S.E., Martin, P.R., Phillips, J.B., Lyczak, R., Hamill, D.R., Swan, K.A., and Bowerman, B. (2000). DNA replication defects delay cell division and disrupt cell polarity in early *Caenorhabditis elegans* embryos. *Dev. Biol.* 228, 225–238.

Etemad-Moghadam, B., Guo, S., and Kemphues, K.J. (1995). Asymmetrically distributed PAR-3 protein contributes to cell polarity and spindle alignment in early *C. elegans* embryos. *Cell* 83, 743–752.

Furuta, T., Tuck, S., Kirchner, J., Koch, B., Auty, R., Kitagawa, R., Rose, A.M., and Greenstein, D. (2000). EMB-30: an APC4 homologue required for metaphase-to-anaphase transitions during meiosis and mitosis in *Caenorhabditis elegans*. *Mol. Biol. Cell* 11, 1401–1419.

Golden, A., Sadler, P.L., Wallenfang, M.R., Schumacher, J.M., Hamill, D.R., Bates, G., Bowerman, B., Seydoux, G., and Shakes, D.C. (2000). Metaphase to anaphase (mat) transition-defective mutants in *Caenorhabditis elegans*. *J. Cell Biol.* 151, 1469–1482.

Goldstein, B., and Hird, S.N. (1996). Specification of the anteroposterior axis in *Caenorhabditis elegans*. *Development* 122, 1467–1474.

Gönczy, P., Schnabel, H., Kaletta, T., Amores, A.D., Hyman, T., and Schnabel, R. (1999). Dissection of cell division processes in the one cell stage *Caenorhabditis elegans* embryo by mutational analysis. *J. Cell Biol.* 144, 927–946.

Guo, S., and Kemphues, K.J. (1996). Molecular genetics of asymmetric cleavage in the early *Caenorhabditis elegans* embryo. *Curr. Opin. Genet. Dev.* 6, 408–415.

Hill, D.P., and Strome, S. (1988). An analysis of the role of microfilaments in the establishment and maintenance of asymmetry in *Caenorhabditis elegans* zygotes. *Dev. Biol.* 125, 75–84.

Hirano, T., Shin-ichi, F., Uemura, T., and Yanagida, M. (1986). Isolation and characterization of *Schizosaccharomyces pombe* cut mutants that block nuclear division but not cytokinesis. *EMBO J.* 5, 2973–2979.

Hird, S.N., and White, J.G. (1993). Cortical and cytoplasmic flow polarity in early embryonic cells of *Caenorhabditis elegans*. *J. Cell Biol.* 121, 1343–1355.

Hung, T.J., and Kemphues, K.J. (1999). PAR-6 is a conserved PDZ domain-containing protein that colocalizes with PAR-3 in *Caenorhabditis elegans* embryos. *Development* 126, 127–135.

Joberty, G., Petersen, C., Gao, L., and Macara, I.G. (2000). The cell-polarity protein Par6 links Par3 and atypical protein kinase C to Cdc42. *Nat. Cell Biol.* 2, 531–539.

Junkersdorf, B., and Schierenberg, E. (1992). Embryogenesis in *Caenorhabditis elegans* after elimination of individual blastomeres or induced alteration of the cell division order. *Roux's Arch. Dev. Biol.* 202, 17–22.

Kamath, R.S., Maruya, M.C., Zipperlen, P., Fraser, A.G., and Ahringer, J. (2000). Effectiveness of specific RNA-mediated interference through ingested double-stranded RNA in *Caenorhabditis elegans*. *Genome Biol.* 2, 1–10.

Kemphues, K.J., Priess, J.R., Morton, D.G., and Cheng, N. (1988). Identification of genes required for cytoplasmic localization in early *Caenorhabditis elegans* embryos. *Cell* 52, 311–320.

Mains, P.E., Kemphues, K.J., Sprunger, S.A., Sulston, I.A., and Wood, W.B. (1990). Mutations affecting the meiotic and mitotic divisions of the early *Caenorhabditis elegans* embryo. *Genetics* 126, 593–605.

McCarter, J., Bartlett, B., Dang, T., and Schedl, T. (1999). On the control of oocyte meiotic maturation and ovulation in *Caenorhabditis elegans*. *Dev. Biol.* 205, 111–128.

Nakaya, M., Fukui, A., Izumi, Y., Akimoto, K., Asashima, M., and Ohno, S. (2000). Meiotic maturation induces animal-vegetal asymmetric distribution of aPKC and ASIP/PAR-3 in *Xenopus* oocytes. *Development* 127, 5021–5031.

Nasmyth, K., Peters, J.M., and Uhlmann, F. (2000). Splitting the chromosome: cutting the ties that bind sister chromatids. *Science* 288, 1379–1385.

O'Connell, K.F., Maxwell, K.N., and White, J.G. (2000). The *spd-2* gene is required for polarization of the anteroposterior axis and formation of the sperm asters in the *Caenorhabditis elegans* zygote. *Dev. Biol.* 222, 55–70.

Pellman, D., and Christman, M.F. (2001). Separase anxiety: dissolving the sister bond and more. *Nat. Cell Biol.* 3, 207–209.

Pfleger, C.M., Lee, E., and Kirschner, M.W. (2001). Substrate recognition by the Cdc20 and Cdh1 components of the anaphase-promoting complex. *Genes Dev.* 15, 2396–2407.

Polinko, E.S., and Strome, S. (2000). Depletion of a Cks homolog in *C. elegans* embryos uncovers a post-metaphase role in both meiosis and mitosis. *Curr. Biol.* 10, 1471–1474.

Rappleye, C.A., Paredez, A.R., Smith, C.W., McDonald, K.L., and Aroian, R.V. (1999). The coronin-like protein POD-1 is required for anterior-posterior axis formation and cellular architecture in the nematode *Caenorhabditis elegans*. *Genes Dev.* 13, 2838–2851.

Reese, K.J., Dunn, M.A., Waddle, J.A., and Seydoux, G. (2000). Asymmetric segregation of PIE-1 in *C. elegans* is mediated by two complementary mechanisms that act through separate PIE-1 protein domains. *Mol. Cell* 6, 445–455.

Riddle, D.L., Blumenthal, T., Meyer, B.J., and Priess, J.R. eds. (1997). *C. elegans II* (Cold Spring Harbor, NY: Cold Spring Harbor Laboratory Press).

Shelton, C.A., and Bowerman, B. (1996). Time-dependent responses to *glp-1*-mediated inductions in early *C. elegans* embryos. *Development* 122, 2043–2050.

Strome, S., and Wood, W.B. (1983). Generation of asymmetry and segregation of germ-line granules in early *C. elegans* embryos. *Cell* 35, 15–25.

Sullivan, M., Lehane, C., and Uhlmann, F. (2001). Orchestrating anaphase and mitotic exit: separase cleavage and localization of Slk19. *Nat. Cell Biol.* 3, 771–777.

Tabuse, Y., Izumi, Y., Piano, F., Kemphues, K.J., Miwa, J., and Ohno, S. (1998). Atypical protein kinase C cooperates with PAR-3 to establish embryonic polarity in *Caenorhabditis elegans*. *Development* 125, 3607–3614.

Tagawa, A., Rappleye, C.A., and Aroian, R.V. (2001). *pod-2*, along with *pod-1*, defines a new class of genes required for polarity in the early *Caenorhabditis elegans* embryo. *Dev. Biol.* 233, 412–424.

Timmons, L., and Fire, A. (1998). Specific interference by ingested dsRNA. *Nature* 395, 854.

Wallenfang, M.R., and Seydoux, G. (2000). Polarization of the anterior-posterior axis of *C. elegans* is a microtubule-directed process. *Nature* 408, 89–92.

Wodarz, A., Ramrath, A., Kuchinke, U., and Knust, E. (1999). Bazooka provides an apical cue for Inscuteable localization in *Drosophila* neuroblasts. *Nature* 402, 544–547.

Zachariae, W., and Nasmyth, K. (1999). Whose end is destruction: cell division and the anaphase-promoting complex. *Genes Dev.* 13, 2039–2058.